Image reconstruction by deterministic compressive sensing with chirp matrices

Kangyu Ni*, Prasun Mahanti, Somantika Datta, Svetlana Roudenko, and Douglas Cochran

Arizona State University, Tempe, USA

ABSTRACT

A recently proposed approach for compressive sensing with deterministic measurement matrices made of chirps is applied to images that possess varying degrees of sparsity in their wavelet representations. The "fast reconstruction" algorithm enabled by this deterministic sampling scheme as developed by Applebaum et al. [1] produces accurate results, but its speed is hampered when the degree of sparsity is not sufficiently high. This paper proposes an efficient reconstruction algorithm suitable for medical images which have good sparsity properties compared to natural images.

Keywords: compressed sensing, chirp, chirp Fourier transform, image reconstruction

1. INTRODUCTION

1.1 The compressed sensing problem

Consider a one dimensional signal x in $\mathbb{R}^N$. An image or any other higher dimensional array can be vectorized into a one-dimensional vector. If the set $\{\psi_i\}_{i=1}^N$, $\psi_i \in \mathbb{R}^N$ is a basis for $\mathbb{R}^N$ then x can be expressed as

$$x = \sum_{i=1}^{N} s_i \psi_i \quad \text{or,} \quad x = \Psi s \tag{1}$$

where Ψ is the matrix $[\psi_1|\psi_2|\dots\psi_N]$ and $s \in \mathbb{R}^N$ is the vector of coefficients. If only k of the coordinates of s are non-zero then the signal x is said to be k-sparse in the system Ψ. The goal in compressed sensing is to be able to reconstruct a k-sparse signal x from only a small number of n linear measurements where $k < n \ll N$ and n is much less than the rate suggested by the Shannon-Nyquist Sampling Theorem. The measured value of the signal x is denoted by $y = [y_1, y_2, \dots, y_n]^T \in \mathbb{R}^n$ and is obtained by computing n inner products between x and a collection of vectors $\{\phi_j\}_{j=1}^n$ as $y_j = \langle x, \phi_j \rangle$. If we define Φ to be the $n \times N$ matrix whose rows are the ϕ_js, then

$$y = \Phi x = \Phi \Psi s = \Theta s. \tag{2}$$

Φ is called the *sensing* or *measurement* matrix and Ψ is called the *sparsifying basis.* Since x and s are equivalent representations of the same signal, recovering s is the same as recovering x. However, the matrix Θ is $n \times N$ making the system in (2) ill-posed. This can be tackled by using the k-sparsity of s and one of the problems in compressed sensing is to construct good sensing matrices Φ which would permit recovery of the signal from only n measurements [2, 3].

1.2 Mathematical Background

If we knew beforehand the exact location of the k non-zero entries of s then we could solve a $n \times k$ over-determined system. Let Θ_{sub} denote the corresponding $n \times k$ matrix. It has been shown that a necessary and sufficient condition for this $n \times k$ system to be well-conditioned is that for any vector v having the same non-zero entries as s, the following holds for some $\epsilon > 0$

$$(1-\epsilon)\|v\| \leqslant \|\Theta_{\text{sub}} v\| \leqslant (1+\epsilon)\|v\|. \tag{3}$$

* Corresponding author

This is the so called *Restricted Isometry Property* (RIP) [4] and in words this says that the the lengths of the vectors v are nearly preserved under Θ_{sub}. In practice one does not know the exact location of the k non-zero entries and this means that for a given Θ the RIP condition has to be verified for the $\binom{N}{k}$ possibilities of Θ_{sub} which is combinatorially complex. So far this issue has been overcome by taking the sensing matrix Φ to be a random matrix for a fixed sparsifying basis Ψ. The entries of the matrix Φ are generated by an i.i.d. random variable like a Gaussian or Bernoulli random variable. Both these cases can be shown to give matrices Θ that satisfy the RIP with very high probability when $\Psi = \mathcal{I}$, the basis of delta spikes. For a Gaussian matrix one needs $n > ck \log(N/k)$ measurements which is much smaller than N [2, 4, 5] . The obvious advantage of using a random matrix with i.i.d. entries is that if the RIP is satisfied for a particular selection of k columns then it should hold with high probability for any other selection of k columns. The reconstruction in this case is by means of solving the following convex optimization problem

$$\min \|\tilde{s}\|_1 \quad \text{such that} \quad y = \Theta \tilde{s}. \tag{4}$$

The optimization problem of (4) can be solved by a method called basis pursuit which has a computational complexity of $\mathcal{O}(N^3)$ and alternatives to basis pursuit like the greedy matching pursuit also have computational complexities that depend on N.

1.3 Deterministic Compressed Sensing Matrices

In recent work, Howard, Applebaum, Searle, and Calderbank have proposed the use of deterministic compressive sensing measurement matrices comprised of "chirps" (i.e., certain families of frequency modulated sinusoids) [1] or second-order Reed-Muller sequences [6]. These matrices come with a very fast reconstruction algorithm whose complexity depends only on the number of measurements n and not on the signal length N. These papers give empirical evidence that compressive sensing matrices formed from these deterministic vectors share certain properties with Gaussian random matrices that make them suitable for compressive sensing. In particular, selecting k columns randomly (i.e., independently from a uniform distribution on all N columns) from the $n \times N$ sensing matrix Φ, yields $k \times k$ gram matrices whose condition numbers are distributed with mean and variance essentially identical to those obtained by using the same procedure on Gaussian matrices. This observation appears to hold over a range of $k < n \ll N$ compatible with those discussed in the compressive sensing literature for random matrices (e.g., [3]). Furthermore, deterministic algorithms for reconstruction of a k-sparse signal vector $x \in \mathbb{C}^N$ from compressive measurements $y = \Phi x \in \mathbb{C}^n$ with $\mathcal{O}(kn \log n)$ computational complexity versus, for example, $\mathcal{O}(knN)$ for ℓ_1 optimization with matching pursuit [1].

In the context of image processing, the roles in which compressive sensing may ultimately prove most useful are still being defined. A key issue is whether various classes of images possess sufficient sparsity to make the use of compressive sensing efficacious. The "one-pixel" camera architecture developed at Rice University [7] is one specialized application that seeks to exploit image sparsity for compressive sampling. Lustig et al. [8] comment that certain medical images are sparse in several senses and make use of this sparsity to enable reconstruction of magnetic resonance (MRI) images from a relatively small number of samples of their Fourier transforms (i.e., in the natural sampling domain for MRI). Candès and Romberg [9] give an example of compressive sensing of a natural image with complex noiselet measurements.

This paper is primarily concerned with whether the deterministic compressed sensing matrices made of chirps as proposed by Applebaum et al. [1] and their associated reconstruction algorithms offer potential in the imaging regime.

2. CHIRP SENSING MATRICES

Fast decoders have been identified for two related classes of deterministic compressive sensing matrices. The first of these, described in [1], is comprised of a family of "chirps" (i.e., frequency modulated sinusoids). The second, introduced in [6], is formed from second-order Reed-Muller sequences [10]. The work presented in the remainder of this paper focuses on the chirp matrices, which will be introduced briefly in the following paragraphs.

A chirp signal of length n with chirp rate r and base frequency m has the form

$$v_{r,m}(\ell) = e^{\frac{2\pi i r \ell^2}{n} + \frac{2\pi i m \ell}{n}}, \qquad r, m, l \in \mathbb{Z}_n. \tag{5}$$

For a fixed n there are n^2 possible pairs (r, m). The full chirp sensing matrix Φ has size $n \times n^2$ and its d^{th} columns is

$$\Phi_{r,m}(\ell) = v_{r,m}(\ell), \qquad j = nr + m \in \mathbb{Z}_{n^2}. \tag{6}$$

Defining $N = n^2$, a k-sparse signal $x \in \mathbb{C}^N$ yields a measurement $y = \Phi x \in \mathbb{C}^n$ that is the superposition of k chirp signals

$$y(\ell) = s_1 e^{\frac{2\pi i r_1 \ell^2}{n} + \frac{2\pi i m_1 \ell}{n}} + s_2 e^{\frac{2\pi i r_2 \ell^2}{n} + \frac{2\pi i m_2 \ell}{n}} + \cdots + s_k e^{\frac{2\pi i r_k \ell^2}{n} + \frac{2\pi i m_k \ell}{n}}. \tag{7}$$

To recover x, Applebaum et al. use FFT to detect one by one the nonzero locations, (r_i, m_i) pairs, whose total computational complexity is $O(kn \log n)$. The magnitudes of the nonzero locations, r_i, are found by solving the associated least squares problem. For reconstructing signals that are sufficiently sparse, this is more efficient than $\ell 1$ minimization with random matrices, which computational complexity is $O(knN)$, in terms of reconstruction speed and reconstruction fidelity.

3. IMAGE RECONSTRUCTION

Despite the success for sparse 1d signals, we observed for real images, this algorithm becomes impractical even for 128×128 and 256×256 images. This is because real images usually are not sufficiently sparse in any transform domain compared to sparse 1d signals. A modified algorithm that is robust to noise can be performed with better image reconstruction fidelity but the computational complexity is $O(kn^2 \log n)$, and therefore, the speed is hampered. For example, a 128×128 image with 10% sparsity in some known domain has 1638 nonzero coefficients. With their reconstruction algorithm, it requires about 1638 iterations and the least squares problems become very large. Moreover, by the rule of thumb, at least approximately 4000 measurements are needed. This implies that only four chirp rates are needed in the sensing matrix, and therefore, the efficiency of finding nonzero locations is not utilized in the imaging regime.

We propose to use discrete chirp-Fourier transform (DCFT) [11] to find the nonzero locations of x and an updated least squares solutions to find the magnitude of these nonzero locations. The former allows detection of several nonzero locations instead of only one nonzero location in each step. The later utilizes calculations of the previous least squares solutions and requires much less memory storage. In detail, the algorithm repeats the following three steps until the samples residual y_0 is sufficiently small. The first step applies DCFT, de-chirps the samples residual with all four chirp rates in the measurement matrix, and then applies FFT

$$w_{r_j}(\ell) = \Big| \mathrm{FFT}\Big(y_0(\ell) \overline{\Phi_{r_j,0}(\ell)} \Big) \Big|, \qquad j = 1, 2, 3, 4. \tag{8}$$

Each obtained magnitude corresponds to a unique pair of chirp rate and frequency. The largest magnitudes are selected and the corresponding pairs (r_i, ℓ) give the nonzero locations of x. The second step solves the magnitudes of these nonzero locations in x by setting up a linear least squares problem, where the matrix A is formed by the chirp matrix columns that correspond to the nonzero locations. The matrix in the current step is expanded from the matrix in the previous step by adding the newly found chirp columns. To solve these least squares problems without treating each problem independently, we use an updated pseudo inverse solution method whose calculations are based on the previous calculations. The pseudo inverse solution of $\min_z ||Az - y||^2$ is

$$z_{sol} = (A^* A)^{-1} A^* y, \tag{9}$$

where * indicates conjugate transpose. Since the current matrix A is obtained by concatenating the newly found columns c with the previous matrix, $A = [\widetilde{A} \quad c]$, finding the inverse of

$$A^* A = \begin{bmatrix} \widetilde{A}^* \widetilde{A} & \widetilde{A}^* c \\ c^* \widetilde{A} & c^* c \end{bmatrix} \tag{10}$$

can be made efficiently by the blockwise inversion formula,

$$\begin{bmatrix} D & E \\ F & G \end{bmatrix}^{-1} = \begin{bmatrix} D^{-1} + D^{-1}E(G - D^{-1}E)^{-1}FD^{-1} & -D^{-1}E(G - D^{-1}E)^{-1} \\ -(G - D^{-1}E)^{-1}FD^{-1} & (G - D^{-1}E)^{-1} \end{bmatrix}, \tag{11}$$

because D^{-1} is known from the previous step and the size of $(G - D^{-1}E)^{-1}$ is small. The calculation of A^*y can also be updated by

$$A^*y = \begin{bmatrix} \widetilde{A}^*y \\ c^*y \end{bmatrix}, \tag{12}$$

where the size of c is much smaller than the size of A. The third step subtracts samples by the linear (their respective magnitudes) sum of the found chirp columns to obtain the new residual y_0.

4. RESULTS

For the experiments, each original image was sparsified by computing its Haar wavelet transform and retaining pre-determined fraction (e.g., 7% or 10%) of its wavelet coefficients, keeping the largest and setting the rest to zero. The image data were sampled with both chirp and noiselet matrices of the same size and reconstructed images were obtained from the samples. Figure 1 shows results for a 128 × 128 pixel angiography image reconstructed using both (our implementation of) noiselet measurements of techniques proposed by Candes and Romberg and the chirp sensing matrix with the reconstruction technique described above. On the left is the ground truth whose sparsity is 10% in the Haar wavelet domain. Both chirp and noiselet took 4099 samples ($\approx$ 25%) for reconstruction. The chirp reconstruction outperformed the noiselet one in terms of the reconstruction error. The error for chirp was -44 dB, which is ten times better than noiselet (-25 dB). The reconstruction error is defined as

$$\text{Error(dB)} = 10 \log_{10} \left[\frac{||x_{\text{actual}} - x_{\text{reconstructed}}||^2}{||x_{\text{actual}}||^2} \right]. \tag{13}$$

In Figure 2, the same is shown for the angiography image with a 256 × 256 pixel resolution. The sparsity of the true image is 7% and 16411 samples ($\approx$ 25%) were used for reconstruction. The chirp reconstruction in this case also outperformed the noiselet. The error for chirp was -32 dB, whereas the error for noiselet was -24 dB. In addition, the computational complexity of finding nonzero locations with DCFT in our experiments is $O(\frac{1}{5}kn\log n)$. This is much smaller than $O(kn^2 \log n)$, by Applebaum et al.'s modified method that is applicable for images.

5. CONCLUSIONS

In conclusion, the modified chirp deterministic method described in this paper provides much better reconstruction algorithm for medical images in terms of the reconstruction errors and computational complexity.

6. ACKNOWLEDGMENT

The authors are grateful for the assistance and advice of Stephen Howard in connection with the work presented in this paper.

REFERENCES

[1] Applebaum, L., Howard, S., Searle, S., and Calderbank, R., "Chirp sensing codes: Deterministic compressed sensing measurements for fast recovery," *Applied and Computational Harmonic Analysis* **26**, 283 – 290 (2009).

[2] Baraniuk, R., "Compressive sensing," *IEEE Signal Processing Magazine* **24**, 118 – 121 (July 2007).

[3] Candès, E., "Compressive sampling," in [*International Congress of Mathematicians*], **III**, 1433–1452, European Mathematical Society, Zürich (2006).

[4] Candès, E., Romberg, J., and Tao, T., "Robust uncertainty principles: Exact signal reconstruction from highly incomplete frequency information," *IEEE Transactions on Information Theory* **52**, 489 – 509 (February 2006).

[5] Candès, E. and Tao, T., "Near optimal signal recovery from random projections: Universal encoding strategies?," *IEEE Transactions on Information Theory* **52**, 5406 – 5425 (December 2006).

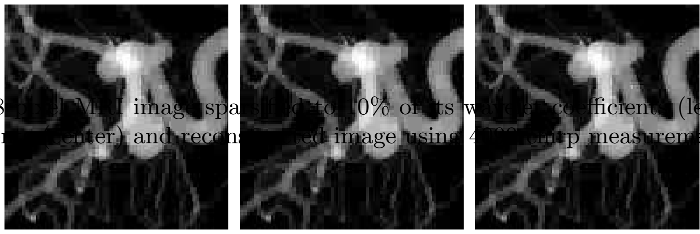

Figure 1. 128 × 128 [illegible] MRI image sparsified to 10% of its wavelet coefficients (left), reconstructed image using 4099 noiselet measurements (center) and reconstructed image using [illegible] chirp measurements (right).

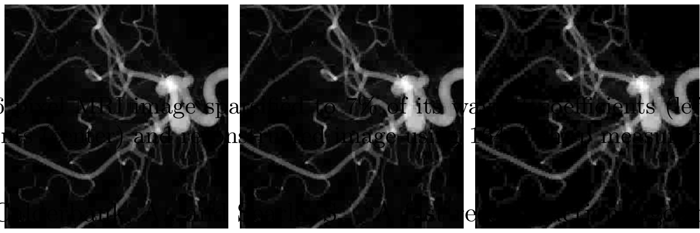

Figure 2. 256 × 256 [illegible] image sparsified to [illegible] of its wavelet coefficients (left), reconstructed image using 16411 noiselet measurements [illegible] and reconstructed image using [illegible] measurements (right).

[6] Howard, S., C[illegible]hm for deterministic compressive sensing using second order Reed-Muller codes," in [*Proceedings of the Conference on Information Sciences and Systems*], (March 2008).

[7] Takhar, D., Laska, J., Wakin, M., Duarte, M., Baron, D., Sarvotham, S., Kelly, K., and Baraniuk, R., "A new compressive imaging camera architecture using optical-domain compression," in [*Computational Imaging IV at SPIE Electronic Imaging*],

[8] Lustig, M., Donoho, D., and Pauly, J. M., "Sparse MRI: The application of compressed sensing for rapid MR imaging," *Magnetic Resonance in Medicine* **58**, 1182 – 1195 (December 2007).

[9] Candès, E. and Romberg, J., "Sparsity and incoherence in compressive sampling," *Inverse Problems* **23**(3), 969 – 985 (2007).

[10] MacWilliams, F. J. and Sloane, N. J. A., [*The theory of error correcting codes*], Elsevier (1976).

[11] Xia, X.-G., "Discrete chirp-fourier transform and its application to chirp rate estimation," *IEEE Transactions on Signal Processing* **48**, 3122 – 3133 (November 2000).

[12] Candès et al., E., "ℓ_1-magic home page." http://www.acm.caltech.edu/l1magic/.

[13] DeVore, R., "Deterministic constructions of compressed sensing matrices," *Journal of Complexity* **23**, 918 – 925 (August 2007).

[14] Donoho, D., "Compressed sensing," *IEEE Transactions on Information Theory* **52**(4), 1289 – 1306 (2006).